SUPPLEMENTARY INFORMATION

Carbon-$Ni_6Co_3Fe_1$ Alloy Hybrid Foil for Electromagnetic Wave Interference Shielding in X-Band and Extremely Low Frequencies

Jihun Lee,[‡a] Yun Seong Cho,[‡a] Dongjoon Rhee,[‡a,b] Hakjeong Kim,[c] Sera Jeon,[d] Dohyun Lee,[a] Jae Won Heo,[a,e,f] Moosung Choi,[g] Ji Hoon Seo,[g] Joon-Young Soh,[g] In Soo Kim,[a,e,f] Sang-Woo Kim,[*d] Dukhyun Choi,[*c,h,i] and Joohoon Kang[*a,e,f]

[a]School of Advanced Materials Science and Engineering, Sungkyunkwan University (SKKU), Suwon 16419, Republic of Korea

[b]Department of Electrical and Systems Engineering, University of Pennsylvania, Philadelphia, PA, USA

[c]School of Mechanical Engineering, Sungkyunkwan University, Suwon 16419, Republic of Korea

[d]Department of Materials Science and Engineering, Yonsei University, Seoul 03722, Republic of Korea

[e]The Nanophotonics Research Center, Korea Institute of Science and Technology (KIST), Seoul 02792, Republic of Korea

[f]KIST-SKKU Carbon-Neutral Research Center, Sungkyunkwan University, Suwon 16419, Republic of Korea

[g]Korea Electric Power Research Institute, 34056 Daejeon, Republic of Korea

[h]Department of Future Energy Engineering, Sungkyunkwan University, Suwon 16419, Republic of Korea

[i]SKKU Institute of Energy Science & Technology (SIEST), Sungkyunkwan University, Suwon 16419, Republic of Korea

‡ Jihun Lee, Yun Seong Cho, and Dongjoon Rhee contributed equally.

*Corresponding authors: joohoon@skku.edu (J. Kang), bred96@skku.edu (D. Choi), and kimsw1@yonsei.ac.kr (S.-W. Kim)

Experimental section

1. Materials

Cobalt sulfate heptahydrate ($CoH_2SO_4 \cdot 7H_2O$, 98%), iron sulfate heptahydrate ($FeH_2SO_4 \cdot 7H_2O$, 98%), nickel sulfate hexahydrate ($NiH_2SO_4 \cdot 6H_2O$, 98%), boric acid (H_3BO_3, 99.5%) and saccharin ($C_7H_5NO_3S$, 98%) were purchased from Sigma-Aldrich. Graphite foil (SIGRAFLEX® Flexible Graphite Foil) was acquired from SIGRAFLEX.

2. Electrochemical deposition

The electrochemical deposition of the NiCoFe alloy was performed using a three-electrode cell consisting of a graphite foil as the working electrode, a graphite rod as the counter electrode, and an Ag/AgCl/KCl (saturated) reference electrode, while an acidic aqueous solution containing 10 mg mL^{-1} of cobalt sulfate heptahydrate, 1.4 mg mL^{-1} of iron sulfate heptahydrate, 28.8 mg mL^{-1} of nickel sulfate hexahydrate, 13.7 mg mL^{-1} of boric acid, and 1.4 mg mL^{-1} of saccharin was used as the electrolyte. Following the electrochemical deposition at 4.5 V for 30–540 min using a potentiostat (SP-50e Potentiostat, BioLogic), the NiCoFe-deposited graphite foil was rinsed with deionized water and dried in a vacuum oven at 60 ℃. To fabricate a large-scale NiCoFe/graphite foil, a two-electrode cell was set up with a graphite foil as the cathode and a graphite plate as the anode. An average current of 20 mA cm^{-2} was applied to the two-electrode cell for 30–540 min using a regulated DC power supplier (DP30-03A, TOYOTECH).

3. X-band EMI shielding measurements

To measure the shielding effectiveness in the high-frequency range (X-band region), samples were positioned between the cylindrical holders, with waveguide-to-coaxial adapters connected to both ends of the holder. Subsequently, a signal analyzer/generator (E5071C ENA Series Network Analyzer 20 GHz, Agilent Technologies) was linked to the waveguide-to-coaxial adapter. Electromagnetic waves in the 8.2–12.4 GHz range were then swept at intervals of 0.021 GHz $step^{-1}$ to determine the shielding effectiveness (dB). Based on the measured scattering parameters (S_{11}, S_{21}, S_{22}, and S_{12}), the reflection shielding effectiveness (SE_R) and absorption shielding effectiveness (SE_A) were calculated using the following equation.

$$SE_R = -10\log(1-R) \tag{S1}$$

$$SE_A = -10\log\frac{T}{1-R} \tag{S2}$$

where R is the reflection ($R = |S_{11}|^2 = |S_{22}|^2$) and T is the transmission ($T = |S_{21}|^2 = |S_{12}|^2$). The total shielding effectiveness (SE_T) was obtained by the sum of SE_R and SE_A.

$$SE_T = SE_R + SE_A \quad \text{(S3)}$$

4. Extremely low-frequency EMI shielding measurements

To characterize the shielding performance of the NiCoFe/graphite composite in the extremely low-frequency region, a box-type shielding system was implemented. Specifically, an electromagnetic field test meter (EMDEX2, EMDEX LCC) was enclosed within a box (10 cm × 10 cm × 10 cm) formed with the composite shield. To apply a uniform magnetic field, a Helmholtz coil with a diameter of 0.9 m and turns of 56 was used, which was in accordance with ASTM-A698/698M-20 standards. After placing the enclosed field test meter at the center of the Helmholtz coil, an AC voltage of 14.4 V was applied to the coil using a function generator (33600A, Keysight) to create a magnetic field with 60 Hz and 10 mG. The shielding performance was evaluated by comparing magnetic field measured before (B_i) and after (B_S) attenuation by the shield. For analyzing the thickness dependence of shielding performance, measurements were conducted while the thickness of the NiCoFe alloy on one side of the shielding box varied from 17 μm to 950 μm. Shielding rate (%) and shielding effectiveness (SE) were calculated as follows.

$$Shielding\ rate\ (\%) = \frac{B_i - B_S}{B_i} \times 100 \quad \text{(S4)}$$

$$SE\ (dB) = 20log\ |B_i/B_S| \quad \text{(S5)}$$

5. Materials characterization

The surface morphology and thickness of the NiCoFe alloy were analyzed using field emission scanning electron microscopy (JSM-7600F, JEOL). For TEM imaging, the NiCoFe/graphite sample was first processed into a TEM specimen based on focused ion beam milling (Helios G4 HX, FEI). The TEM specimen was then characterized using a transmission electron microscope (Titan 80-300, FEI) to acquire SAED patterns and EDS mapping data for crystal structure and elemental distribution analyses. The XRD patterns of graphite and NiCoFe/graphite composite samples were obtained using an X-ray diffractometer (Aeris, Malvern Panalytical) equipped with a Cu Kα source (wavelength: 1.54 Å) over the 2θ range of 10–68°. For XPS analysis, data was collected using X-ray photoelectron spectroscopy (Nexsa, ThermoFisher scientific), enabling the analysis of bonding states and elemental composition of the NiCoFe alloy. The sheet resistance of the samples was measured using a 4-point probe (CMT-SR2000N, Advanced Instrument Technology). The magnetization–magnetic field strength (*M–H*) curves were measured at 298 K using a vibrating sample magnetometer (DynaCool-14, Quantum Design, Inc.) from -2.5 to 2.5 T at a scan rate of 0.00165 T s^{-1}.

6. Thermal conductivity measurements

To determine the thermal conductivity, three physical properties were measured: thermal diffusivity, density, and specific heat capacity. The thermal diffusivity was obtained by using a laser flash apparatus (LFA 467 HyperFlash, NETZSCH). The density was measured using a

weighing device (QUINTIX224-1SKR, Sartorius). The specific heat capacity was characterized using a differential scanning calorimetry (DSC 214 Polyma, NETZSCH).

7. Mechanical properties measurements

The elastic modulus and ultimate strength of the pristine and NiCoFe-deposited graphite foils were measured using a universal testing machine (AGX-20kNVD with a 50-N load cell, SHIMADZU) to investigate the effect of the NiCoFe film on the mechanical properties of the shield.

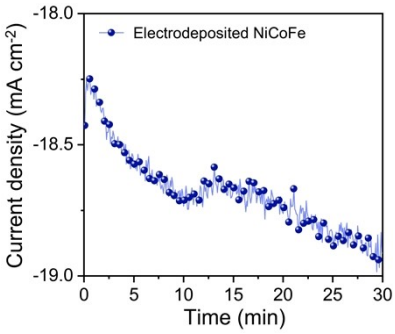

Fig. S1. Chronoamperometry measurements of electrodeposition process up to 30 min.

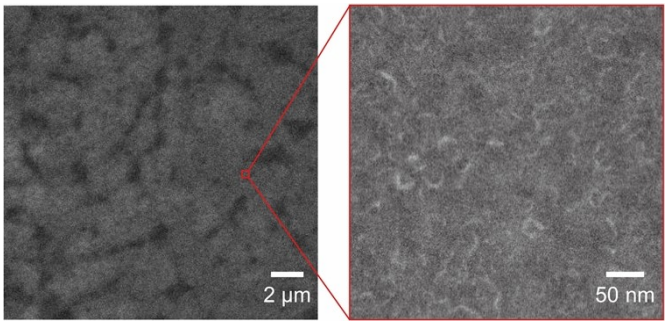

Fig. S2. SEM image of NiCoFe alloy film.

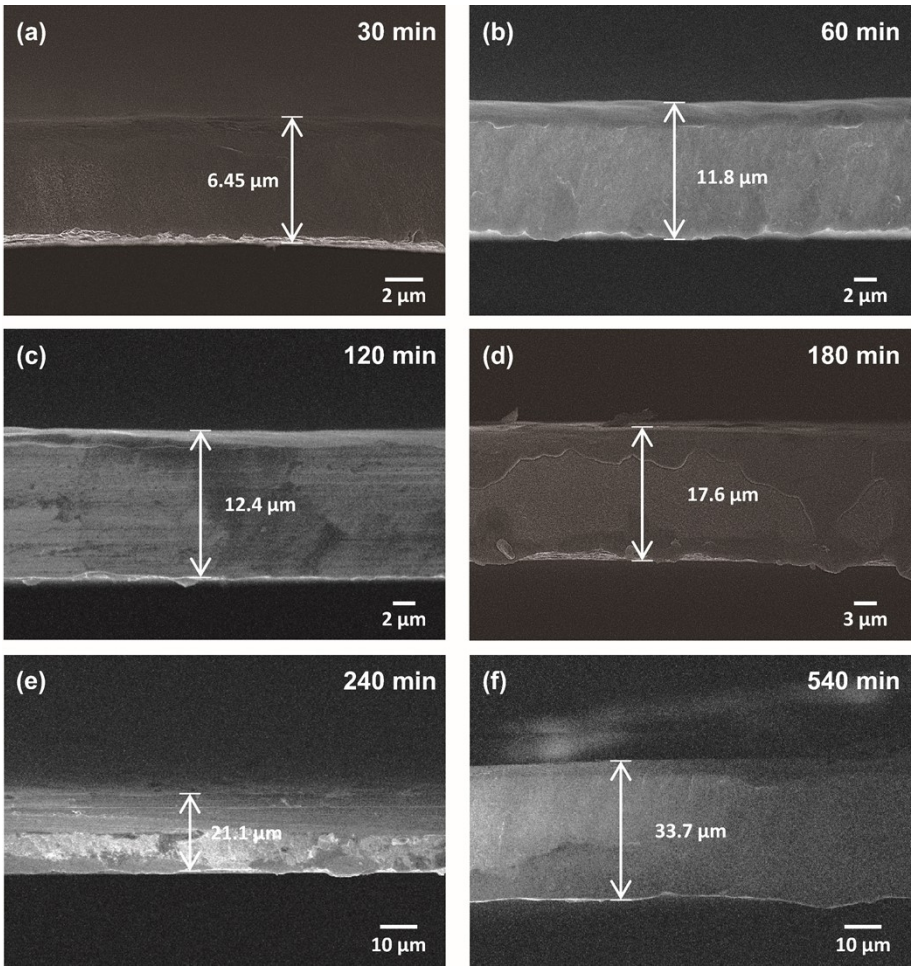

Fig. S3. Cross-sectional SEM images and thicknesses of electrodeposited NiCoFe alloy films. Samples fabricated with deposition times of **(a)** 30 min, **(b)** 60 min, **(c)** 120 min, **(d)** 180 min, **(e)** 240 min, and **(f)** 540 min, respectively.

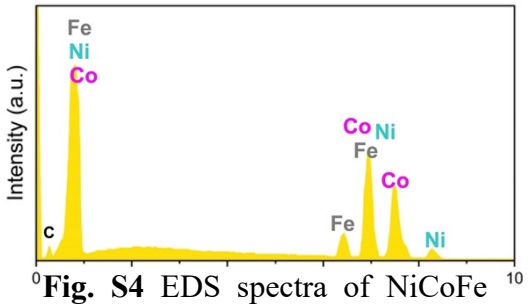

Fig. S4 EDS spectra of NiCoFe film.

Element	Weight%	Atomic%
Fe K	10.05	10.52
Co K	31.9	31.7
Ni K	58.0	57.8
Total	100	100

Table S1. Weight and atomic ratios of NiCoFe film on graphite foil determined by TEM EDS analysis.

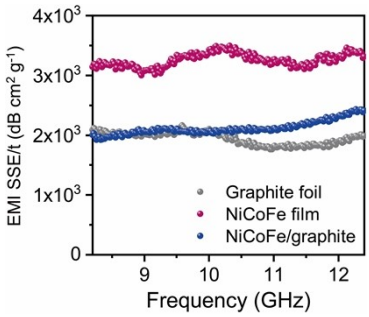

Fig. S5. Absolute shielding effectiveness of graphite foil, NiCoFe alloy film, and NiCoFe/graphite composite.

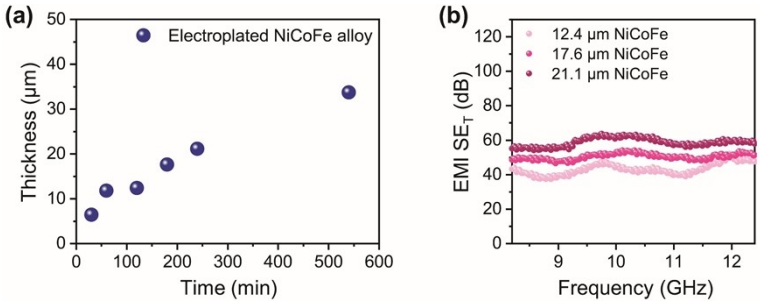

Fig. S6. EMI shielding effectiveness of NiCoFe alloy films. **(a)** Relationship between the electrodeposition time and thickness of the NiCoFe alloy. **(b)** Total shielding effectiveness of the NiCoFe alloy depending on the thickness.

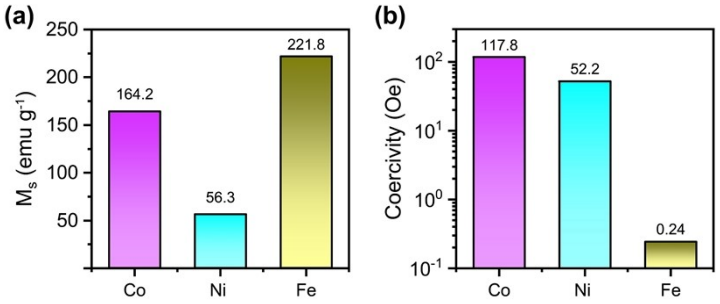

Fig. S7. Magnetic properties of Co, Ni and Fe powders. **(a)** Saturation magnetization. **(b)** Coercivity.

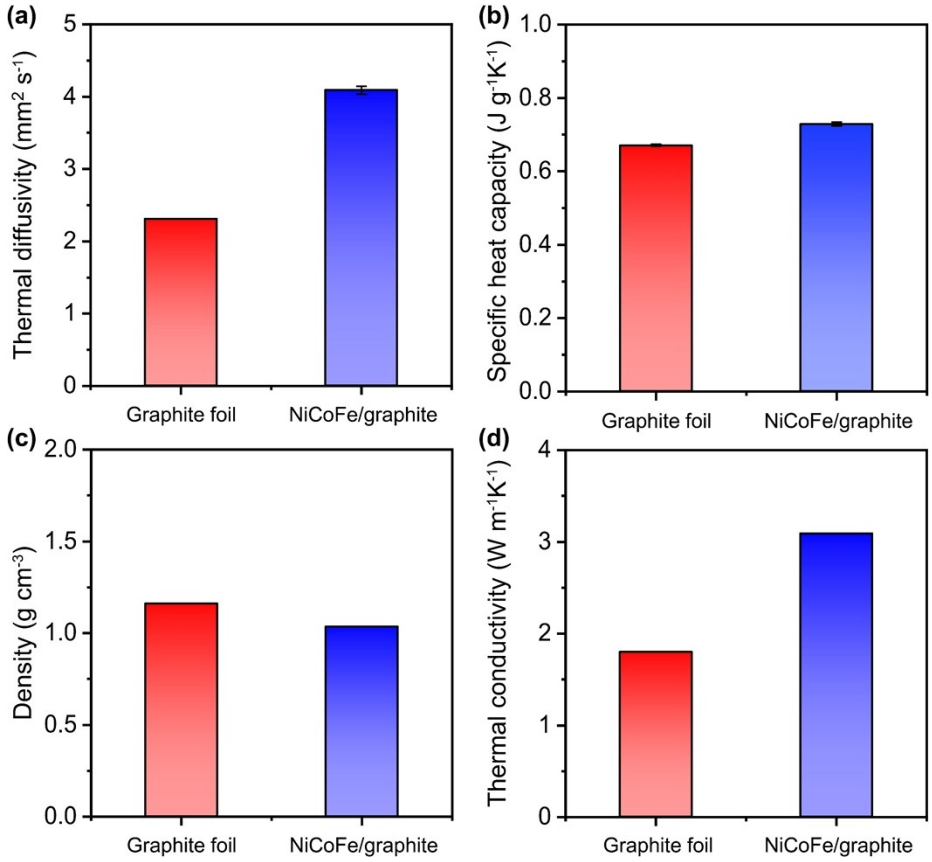

Fig. S8. Thermal properties of graphite and NiCoFe/graphite foils. **(a)** Thermal diffusivity. **(b)** Specific heat capacity. **(c)** Density. **(d)** Thermal conductivity.

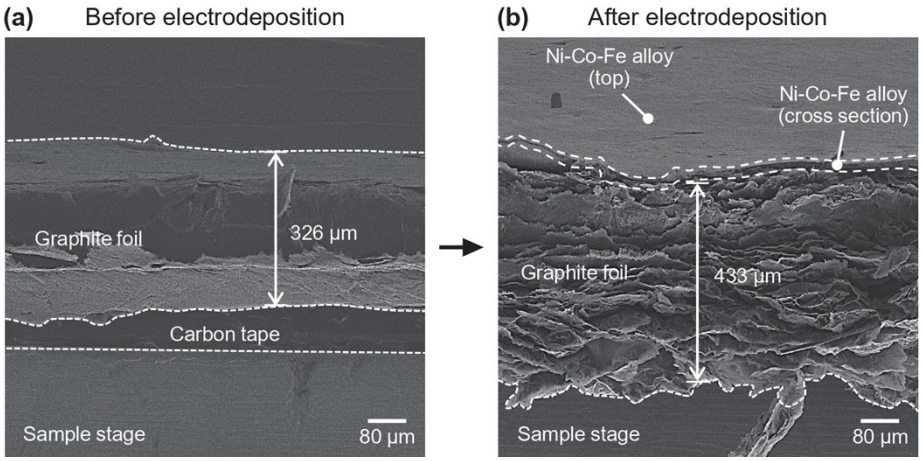

Fig. S9. Cross-sectional SEM images of the graphite foil **(a)** before and **(b)** after the electrodeposition process.

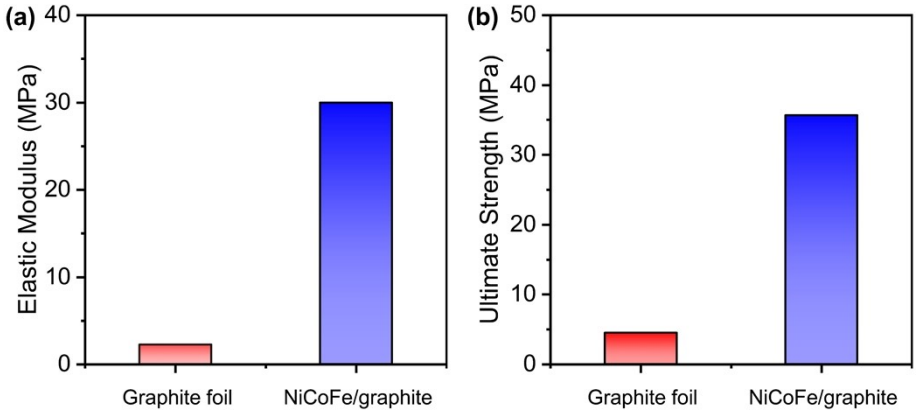

Fig. S10. Mechanical properties of graphite and NiCoFe/graphite foils. **(a)** Elastic modulus. **(b)** Ultimate strength.